Ilass 2013

Influence of nozzle hole eccentricity on spray morphology

Andreas Schmid[1], Beat von Rotz[1], Reiner Schulz[1], Kai Herrmann[1], German Weisser[1], Rolf Bombach[2]
1: Wärtsilä Switzerland Ltd., Winterthur, Switzerland
2: Paul Scherrer Institute, Villigen PSI, Switzerland

Abstract

Large marine two-stroke diesel engines have an injector geometry, which differs substantially from the configurations used in most other diesel engine applications, as the injector orifices are distributed in a highly non-symmetric fashion. In order to experimentally assess the impact of key features of such orifice arrangements on spray morphology, orifice eccentricity relative to the injector axis in particular, a dedicated test setup has been realised, including the development and application of tailor-made data processing routines. The high-speed camera recordings of the Mie-scattering data obtained simultaneously for two perpendicular views of single sample sprays have been analysed in terms of spray tip penetration and spray angle as well as with respect to the orientation of the spray. These analyses confirm the complex three-dimensional structure of sprays at such conditions: They are in fact far from rotationally symmetric – specifically when high levels of eccentricity apply – and the actual orientation of their axis in such cases clearly deviates from the nominal one, normally assumed to be in line with the orifice axis. These deflections are in the range of 10° and they apply not only in the direction of the eccentricity but also perpendicular to it. Additional effects arise from the geometric configuration of the central bore of the injector, upstream of the orifice, and when varying the injection pressure. In the case of high eccentricity, moreover, a clear pattern can be discerned in the initial evolution of the spray deflection: Starting from a slight deflection in the direction of the eccentricity, the spray axis moves first to its nominal direction and then gradually changes orientation again towards the level of stabilisation.

Introduction

In contrast to other diesel engine applications, large two-stroke marine diesel engines are equipped with at least two injectors, which are protruding from the side of the cylinder head into the combustion chamber. The fuel is injected into a cylinder charge characterised by significant swirl levels, via typically five orifices per injector. As a consequence, the injectors are highly non-symmetric, in contrast to the designs typically used in all other types of diesel engines. Figure 1 shows a sample design of the tip of such injector.

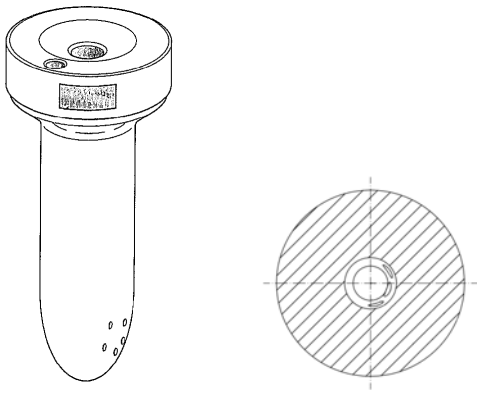

Figure 1 Sample design of typical fuel injector tip (left), cross-section through orifice region (right).

In order to achieve an optimum distribution of the fuel in the combustion chamber, the individual orifices are normally sized differently and covering only a relatively small range of angles on a plane perpendicular to the axis of the injector. This small range of angles of the orifices requires the suitable selection of their arrangement without unnecessarily prolonging the injector tip as this would result in excessive heating of the (uncooled) injectors, thus reducing their lifetime. On the other hand, fundamental mechanical stability requirements dictate a minimum distance between the orifices. In order to meet those requirements, the design of individual orifices involves non-negligible levels of eccentricity of the orifice axis relative to the injector axis.

Preliminary investigations by means of LES simulations [1] showed that the liquid core is no longer symmetrical in case of eccentric arrangements of the nozzle hole with respect to the central bore of the injector. First pre-tests [2] verified experimentally that nozzle hole eccentricity has a non-negligible effect on spray morphology. Based on these findings, the present, more extensive study was initiated.

Experimental setup

The investigations were performed making use of the Spray Combustion Chamber (SCC), an optically accessible constant volume chamber of dimensions representative of smaller two-stroke as well as larger four-stroke marine diesel engines (Ø500x150mm) [3] and validated at conditions typical of those engines [4].

Figure 2 shows a schematic of the test facility, illustrating the working principle of the experimental setup: A pressure vessel equipped with fast opening valves feeds process gas via a heater, the so-called regenerator, into the SCC. Pressure and temperature levels as well as swirl in the spray combustion chamber are adjustable by changing accumulator pressure and/or duration of the blow down process and heater core temperature. By starting the injection with sufficient delay after the end of the blow-down process, due to the continuous decay of the swirl, quasi-quiescent conditions can also be realised.

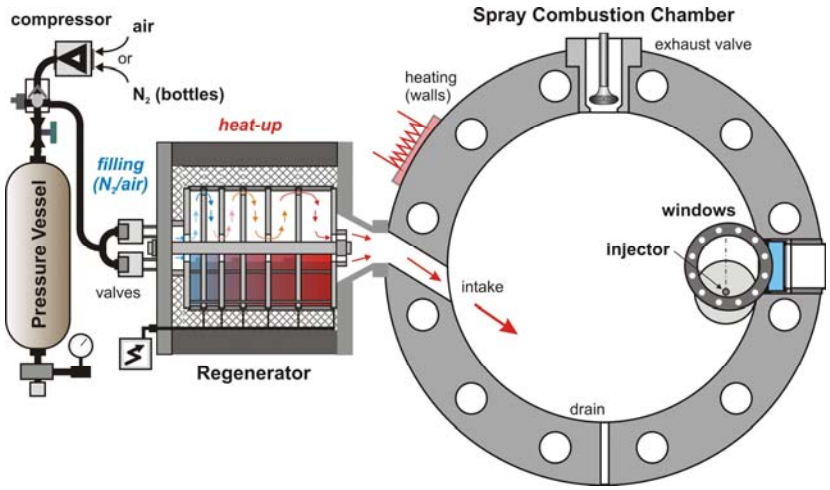

Figure 2 Spray Combustion Chamber schematics.

Figure 2 also illustrates the specific injector positioning and optical access arrangement options devised for this purpose: In contrast to most earlier tests, where the morphology of sprays has been analysed from a perspective perpendicular to the injector axis, the current experiments specifically target the observation of the spray in a direction parallel to the axis of the injector. Hence, whereas the earlier tests made use of an improved shadow-imaging technique [5], which is relying on the availability of optical access options in front and in the back of the item under investigation, the Mie scattering technique had to be applied in this context. However, in order to obtain additional information on the three-dimensional behaviour of the spray, the spray was simultaneously observed from the side by means of a second window and high-speed camera. A Nd:YLF-Laser was used for illuminating the liquid phase of the spray. The scattered light was then captured with two high speed cameras operated at 20 kHz, which were located in front and on the side of the spray.

Figure 3 shows the optical setup, with the injector mounted on the back side of the SCC and the two cameras in the front and on the side of the chamber. Camera one was flanked by the two illumination beams: With the help of a beam splitting cube, the laser light was separated into two part-beams which were then guided past both sides of the front camera. Using such setup resulted in a more homogenous illumination of the spray and therefore an easier detection of possible asymmetry in the spray pattern.

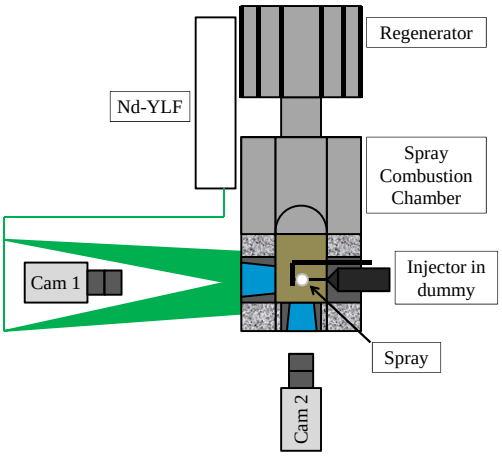

Figure 3 Optical setup at the Spray Combustion Chamber (SCC).

In order to enable the investigation of the isolated effect of orifice eccentricity on spray morphology, a special injector configuration has been developed, shown in Figure 4 (right photograph): The theoretical direction of the spray originating from the single orifice located at a certain eccentricity with respect to the axis of the injector is indicated by the red arrow. In order to realise the same flow conditions at the inlet of the injector as in a five-hole injector, a second orifice with correspondingly enlarged flow area is located at sufficiently large distance downstream of the first orifice for avoiding any disturbance of the flow into the latter. Any potential impact of this second orifice on the processes inside the SCC is avoided by redirecting the fuel flowing past it into a plenum outside the SCC (black arrows in right

photograph of Figure 4). The injector was positioned in the back cover, via an adapted dummy device, which was mounted instead of a window. The left photograph in Figure 4 gives an impression of the complete assembly of this "injector in dummy" configuration, including the mounted injector, the nozzle with the eccentric single-hole and the fuel discharge system.

Figure 4 additionally illustrates the main design parameters varied in this investigation: A frontal cut of the nozzle (view A-A) visualizes the eccentricity *e*, the nozzle hole diameter *d* and the diameter *D* of the main bore through the injector tip. Sectional view B-B shows the inner geometry of the nozzle tip. Two types of designs were tested, in consideration of the expected different conditions for the flow approaching the nozzle hole: Whereas Type 1 was designed such that the fuel flows towards the orifice in a more or less undisturbed way almost perpendicular to its axis, Type 2 is characterised by a backward facing step upstream of the nozzle hole. The intention was to generate strong turbulence at the entrance to the nozzle hole.

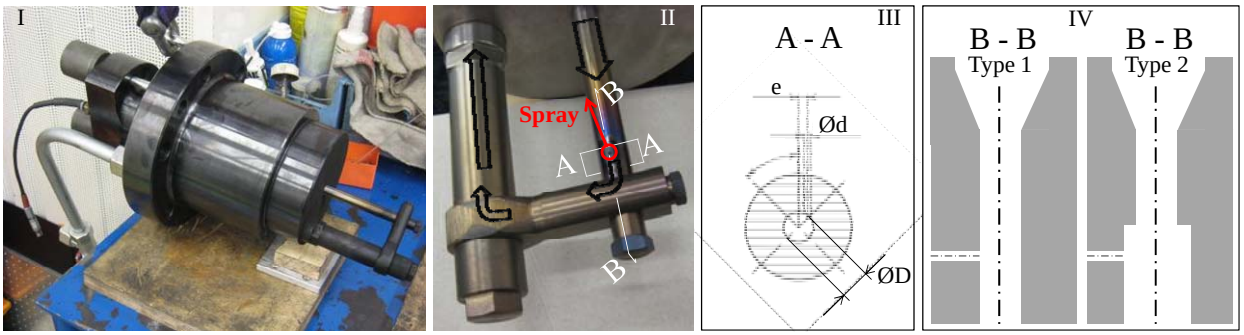

Figure 4 Injector design: Complete "injector in dummy" assembly (I), close-up view of injector arrangement including flow directions (II), injector frontal sectional view (III) and transversal sectional view (IV)

Results and Discussion

The present investigations were applied with air as the process gas at chamber conditions of 4 MPa and 400 K in the absence of swirl. Table 1 gives an overview on the different measurement points. Beginning with the reference case (Case # 1: Type 1 nozzle, injection pressure 80 MPa, eccentricity $e = 0$) the pressure of the light fuel oil in the rail has been varied from 60 to 100 MPa. The eccentricities *e* have been normalised to $e = e_{real} / (D/2 - d/2)$ and have been varied from 0 up to 0.8.

Case #	1	2	3	4	5	6	7	8	9	10	11	12	13	14	15
Normalised eccentricity	0	0	0	0.80	0.80	0.80	0.40	0.40	0.40	0.59	0.59	0.59	0.29	0.29	0.29
Rail pressure [MPa]	80	100	60	60	80	100	100	80	60	100	60	80	80	100	60
Nozzle type	1	1	1	1	1	1	1	1	1	2	2	2	2	2	2

Table 1 Overview of measurement conditions

Qualitative spray behaviour

The qualitative impact of the eccentric arrangement of an orifice with respect to the axis of the central bore of the injector on the fully established spray is illustrated in Figure 5: Whereas, in the absence of eccentricity, the actual axis of the spray coincides with the theoretical one, the spray is significantly deflected from the orifice axis with high eccentricity. The deflection is in the range of 10°, against the direction of the eccentricity.

An interesting effect can be observed during the initial phase of injection, before the spray is fully developed, specifically at high eccentricity (see Figure 6): Initially, a small portion of the fuel seems to leave the orifice at low velocity in a direction opposite of the direction of the eccentricity and the later stabilisation of the spray. In the course of the further development, the spray then first seems to follow the theoretical axis defined by the orifice direction and is then gradually more and more deflected against the direction of the eccentricity (towards the nozzle bore), before it finally stabilises.

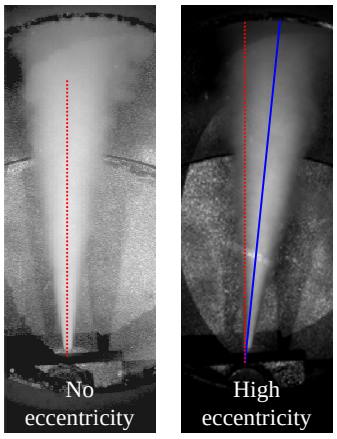

Figure 5 Spray deflection due to eccentricity.

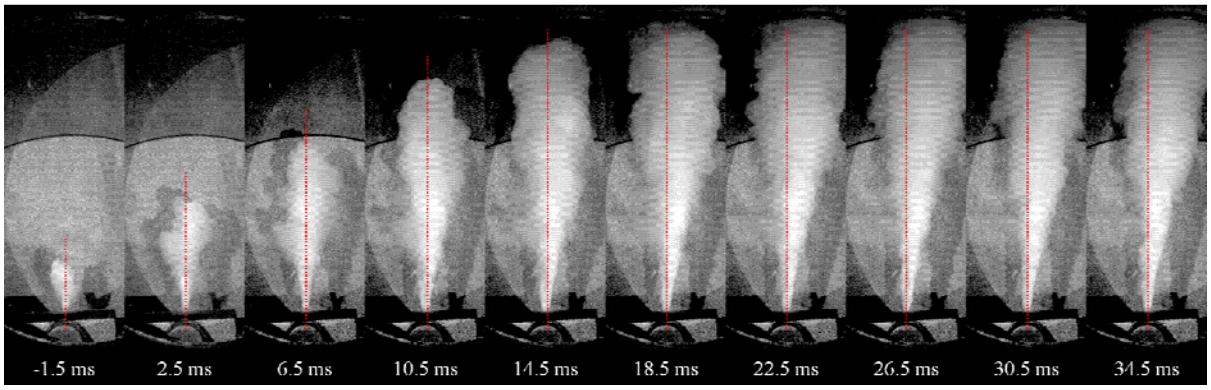

Figure 6 Temporal evolution of spray at maximum eccentricity.

Data processing for quantitative analyses

The presence of a metallic surface on the back of the cell poses significant challenges to the automation of image processing: The strong reflections made it virtually impossible to distinguish between spray and background merely on the basis of intensity differences. Therefore, a sophisticated filtering method had to be devised, which was subsequently applied to all individual images. Figure 7 gives an overview of the different steps:

The raw image (a) was first filtered with a so called range-filter. Due to the optically rough metal surface, the background showed different frequency behaviour compared to the much smoother surface of the illuminated spray (b). In order to amplify these differences the image was then divided by an average-smoothed version of the image. This led to a distinct separation between the spray plume and the background (c), which could then easily be filtered via a threshold (d). With the help of this image, both the spray penetration and the spray angle have been determined. This image was then defined as the region of interest, which was applied again to the raw image, resulting in the spray plume without any disturbances (e). This image was finally processed with a strong average filter. At a distance of 40 times the nozzle-hole diameter ($40 \cdot d_0$), the angle between the nozzle hole symmetry axis (nominal spray axis) and the deflected spray plume axis was determined. For this purpose, the intensity distribution across the spray plume was taken. The maximum of this distribution was then defined as the spray axis.

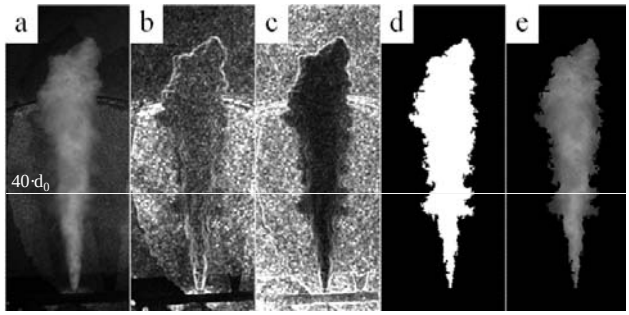

Figure 7 Image processing steps.

This analysis was performed for each image of each measurement series of each realisation of each individual case. Note that, per case, ten high speed recordings were acquired. As an example, Figure 8 shows the spray

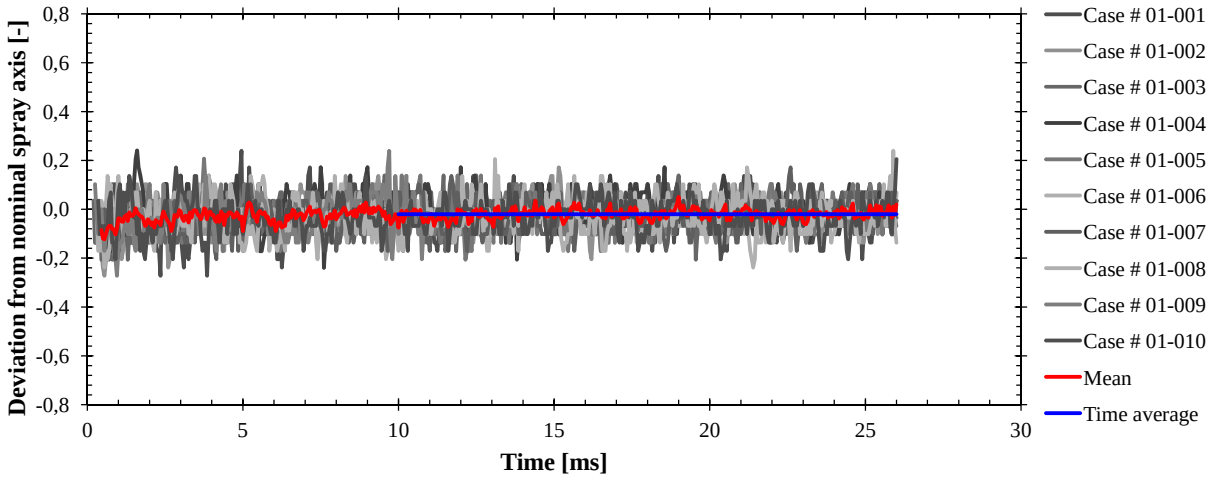

Figure 8 Spray deflection from nominal spray direction for the reference case with the mean value on top and the single value calculated from 10 to 26 ms. Time is set to zero for the arrival of the spray at $40 \cdot d_0$.

deflection from the nominal spray axis for the ten realisations of the reference case over a time period of 26 ms, with the start time defined as the timing of the arrival of the spray at the measuring location.
The curve of the averaged values over all ten measurements is plotted on top of the individual experiments (red curve). With the help of this mean value data plot two phases can be determined: During a first phase, up to about ten milliseconds, the axis of the spray is varying quite significantly. After that period, the spray axis has been established at a stable position, around which it continues fluctuating until the end of injection. The range for this fluctuation is within the standard deviation of all ten measurements, which is about 0.82° for the reference case during this second (stabilised) phase. The time average of the mean value data of all ten measurements for the period after stabilisation (at about 10 ms – blue line) is then used for comparing the results of different cases. For the reference case shown here, this single value characterising the spray deflection from the nozzle axis is about zero.

Spray tip penetration

The penetration of the spray tip as a function of time for different levels of eccentricity (and nozzle types) at otherwise identical conditions (chamber pressure and temperature, rail pressure = 80 MPa) is shown in Figure 9. Note that the region below ca 10 mm from the orifice exit had to be excluded from the analysis for two reasons: Firstly, this region is partly shielded from the observation by the specific setup associated with the redirection of the portion of the fuel corresponding to the quantity injected via the other four orifices in a production injector. Secondly, minimum area coverage by the spray is required for recognition by the automated image processing.

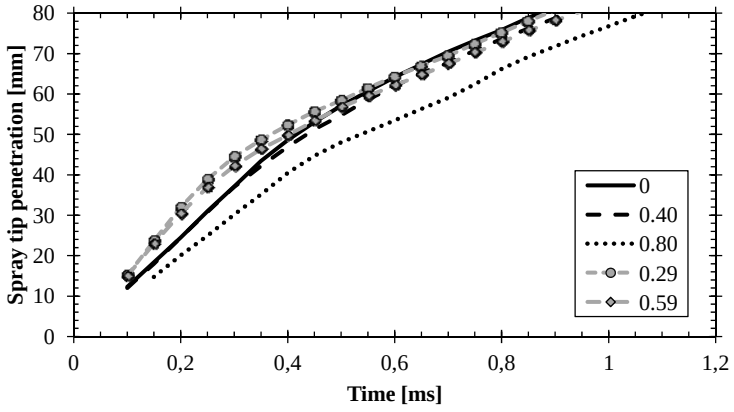

Figure 9 Spray tip penetration for the two nozzle types (Type 1 in black, Type 2 in grey) at different eccentricities.

The spray penetration of the reference case (Type 1 injector without eccentricity) behaves as expected from literature ([6], [7]) and earlier own investigations ([5], [8]): A linear phase up to the spray break-up time / length is followed by a second phase, during which the penetration increases with time according to a square root function relationship.
Increased eccentricity slightly reduces the velocity during the linear phase and slows down spray tip penetration around the break-up length and during the second phase. In the large eccentricity case, the linear velocity is already clearly reduced. Whereas the break-up length is not influenced by different degrees of eccentricity, the second phase of the penetration shows an unsteady behaviour with higher eccentricity and also the shape is different: The second phase becomes more linear instead of the root shape as in the reference case. The reason for this particular behaviour is at present not fully understood.
The grey curves in Figure 9 show that the nozzle design (and the associated flow conditions at the inlet of the orifice), have a strong effect on spray penetration. Compared to the reference case, with Type 2 nozzles, the fuel exits the orifice at higher velocity until it reaches the break-up length. Apparently, it then undergoes a stronger reduction of spray tip velocity. The reason for all this is suspected in the reduced velocity due to the sudden increase in flow area within the nozzle (backwards facing step before the orifice, compare Figure 4 on the right side). This reduction in flow velocity (about 60%) increases the static pressure in the region of the orifice compared to the level of Type 1 nozzles, which, together with the different turbulence levels at the orifice inlet must be expected to have an impact on the formation and propagation of the spray. Unfortunately, the data available do not allow a conclusive statement on any potential effect of eccentricity.

Spray angle

Figure 10 shows the time averaged spray angles for both nozzle types as a function of eccentricity. The upper data plot shows the “front view” spray angle (observed with camera 1) and the lower shows the “side view” spray angle (observed with camera 2).
For the reference case, the values of the “front view” and “side view” angles are at 20.5° and 21.9°, respectively, which clearly indicates that the spray is not rotationally symmetric with respect to its axis, but rather characterised by an elliptic shape. This had to be expected as a consequence of the change of direction of the flow by 90° at the inlet of the orifice, which is resulting in a significantly more pronounced distribution of all key parameters in direction of the injector axis compared to the transversal direction.

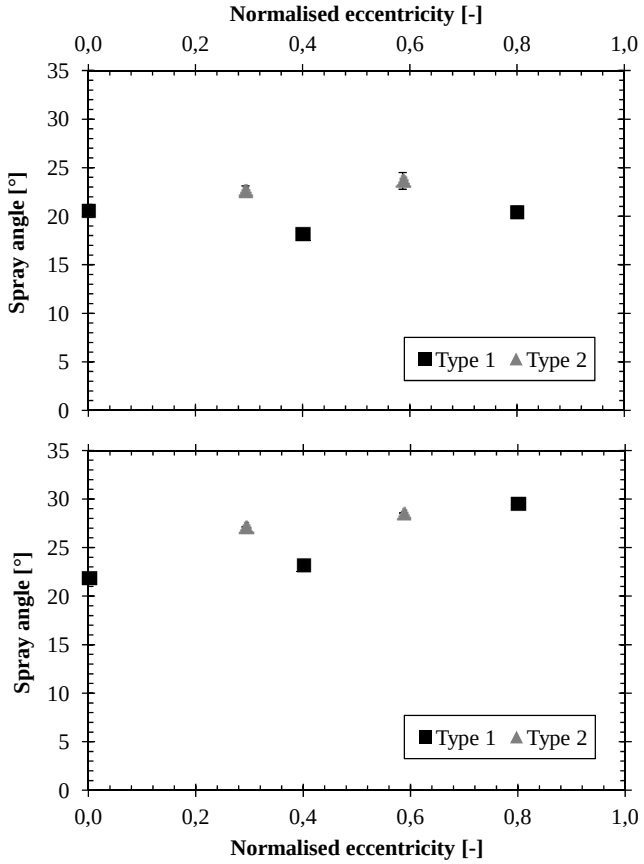

Figure 10 Spray angles in front (top) and side (bottom) views as a function of eccentricity.

It is worthwhile noting that, with Type 1 nozzles, the "front view" spray angle does not vary much as a function of eccentricity: Whereas the angle at intermediate eccentricity appears to be slightly lower than the one in the reference case, it is virtually back at the same level with the maximum eccentricity case.

In contrast, the "side view" angle shows a clear trend towards higher values with increasing eccentricity. Whilst the increase at intermediate eccentricity can be considered as sort of balancing the moderate decrease of the corresponding "front view" value, the level achieved at maximum eccentricity is significantly higher. Note that the elliptic structure of the spray is becoming clearly more pronounced with increasing eccentricity: Starting from a level of 1.07, the ratio of the angles observed in side and front views, respectively, increases to 1.28 at intermediate and 1.44 at high eccentricity level.

In the maximum eccentricity case, the average spray angle is clearly increased when compared to the reference and intermediate eccentricity cases, which is sort of consistent with the reduced penetration observed in this case (compare Figure 9).

For Type 2 nozzles, largely similar considerations apply; though, trendwise, the spray angles with those nozzles are generally higher than with the Type 1 variants. This was basically expected as a consequence of the anticipated higher turbulence level at the inlet of the orifice. The sprays are also clearly non-symmetric and both the "front view" and "side view" angles seem to increase linearly as a function of eccentricity.

Spray deflection (stabilised spray)

In Figure 11, the spray deflection from the nominal axis is plotted as a function of eccentricity for Type 1 and Type 2 nozzles. The data have been normalised by referencing them to the maximum deviation measured at reference conditions (Type 1 nozzle, rail pressure 80 MPa). The upper diagram shows the radial deflection determined from the front view images (camera 1), whereas the lower diagram includes similar data for the "axial" deflection obtained from the side view images (camera 2). Note that the analysis procedure in this case has been slightly different, due to the fact that the spray was illuminated only from the front (compare Figure 3) such that the intensity distribution analysis might have lead to erroneous results. Instead, the spray axis is set at the middle of the contour of the spray. The subsequent identification of the stabilised spray angle from the data obtained from the individual images of the individual realisations of the respective cases then followed again the procedure outlined above.

Whereas the deviation of the actual from the nominal spray axis is close to zero in the reference case, sprays originating from Type 1 nozzles at increasing levels of eccentricity are characterised by progressively rising radial deflection s, in direction of the eccentricity e, a behaviour, which can be approximated by the function: $s = (1.25 \cdot e)^{2.5}$. With Type 2 nozzles, the effect seems to be less pronounced – in this case, the radial deflection rather follows a linear relationship with eccentricity: $s = 0.9 \cdot e$.

It is interesting to note that the deflection is not limited to the direction of the eccentricity (see axial deflection graph in Figure 11): Whereas the actual spray orientation in the reference case again coincides well with the nominal one (no deviation from the orifice axis), we observe a non-negligible deflection of the spray in direction of the flow in the central bore of the injector, specifically with the Type 2 nozzle cases and at high eccentricity with the Type 1 nozzle. In the case of the Type 2 nozzles, there seems to be no significant impact of eccentricity, at least not within the range considered here. The fact that the deflection with this type of nozzle is more pronounced than with the Type 1 variants at similar eccentricity could be attributed to the fact that the flow conditions at the inlet of the orifice are expected to be substantially different due to the effect of the recirculation region establishing at the backward facing step upstream of the orifice. The axial deflection of the spray at

maximum eccentricity with the Type 1 nozzle is at almost 30% of the radial deflection at the same conditions, which is again a strong indication of the pronounced three-dimensional character of sprays generated at such conditions.

For each of the presented cases, a rail pressure variation has been performed. Whereas the general spray behaviour in terms of penetration and angle has been in accordance with expectations (not discussed here in detail for the sake of brevity), there is an additional effect on the deflection of the spray. Figure 12 shows the nominal deflection in radial direction for both nozzle types obtained in tests at their respective maximum eccentricity (0.8 for Type 1, 0.59 for Type 2) as a function of rail pressure, which has been varied between 60 and 100 MPa.

Both nozzle types show similar behaviour: The spray deflection is clearly reduced with increased rail pressure, with the effect being relatively more pronounced in the case of the Type 2 nozzles. One can assume that the higher momentum of the spray outweighs the effects responsible for the deflection of the spray such as non-symmetric flow characteristics at the orifice inlet and non-uniform friction distribution inside the orifice due to the larger surface area on the side of the eccentricity. As the latter is of lower relevance in the Type 2 nozzle case, the flow distribution effects can be suspected to be dominant.

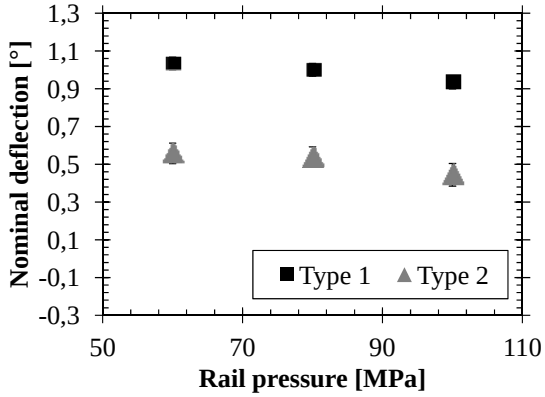

Figure 12 Influence of rail pressure on radial spray deflection at the respective maximum eccentricity.

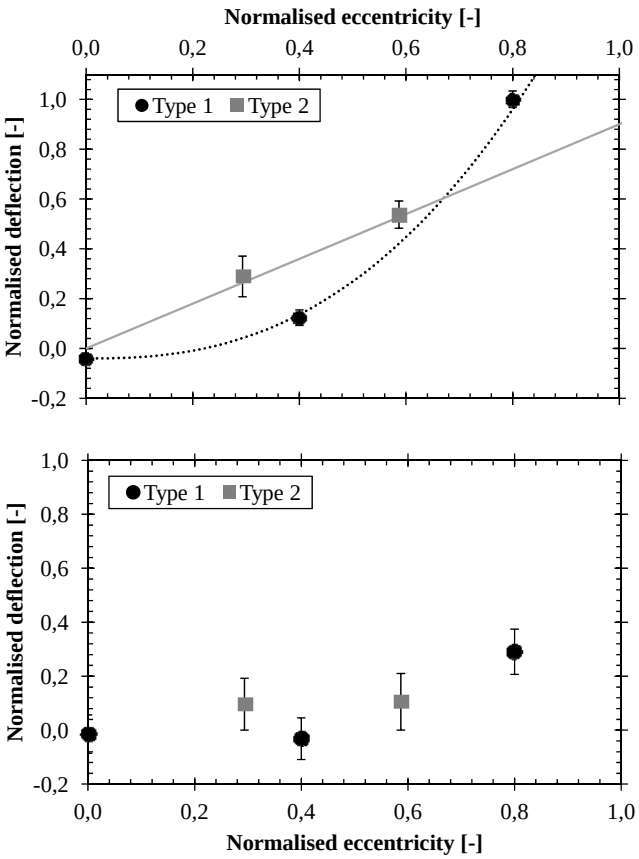

Figure 11 Axial (top) and radial (bottom) deflection of stabilised sprays from their nominal axis as a function of eccentricity.

Transient spray deflection behaviour

The highly transient evolution of the spray deflection during the initial phase illustrated in Figure 6 has also been analysed quantitatively. The left diagram in Figure 13 shows the deviation of the actual spray axis orientation from the nominal axis as a function of time for three levels of eccentricity with Type 1 nozzles, during the first four milliseconds.

With the reference and intermediate eccentricity cases, we observe quite some fluctuations; however, no clear pattern can be recognised. This is different in the high eccentricity case, where, starting from a slight deflection in the direction of the eccentricity, the spray axis moves first to its nominal direction and then gradually changes orientation again towards the level of stabilisation.

Injection pressure also has an impact on this initial behaviour: The right diagram in Figure 13 compares the evolution of the spray axis orientation during the same first four milliseconds for the 60, 80 and 100 MPa rail pressure cases. The general pattern is similar in all the cases; however, there are differences in the minimum deflection levels observed and also in the speed at which the orientation approaches the stable deflection level: On the one hand, with high injection pressure, the spray axis is no longer reaching its nominal direction. On the other hand, with reduced injection pressure, the stabilisation process takes considerably longer.

The background for this particular behaviour is at present not well understood. It requires further and more in-depth investigations, specifically into the transient fluid-dynamic effects governing the flow inside the injector in general and inside the orifice in particular.

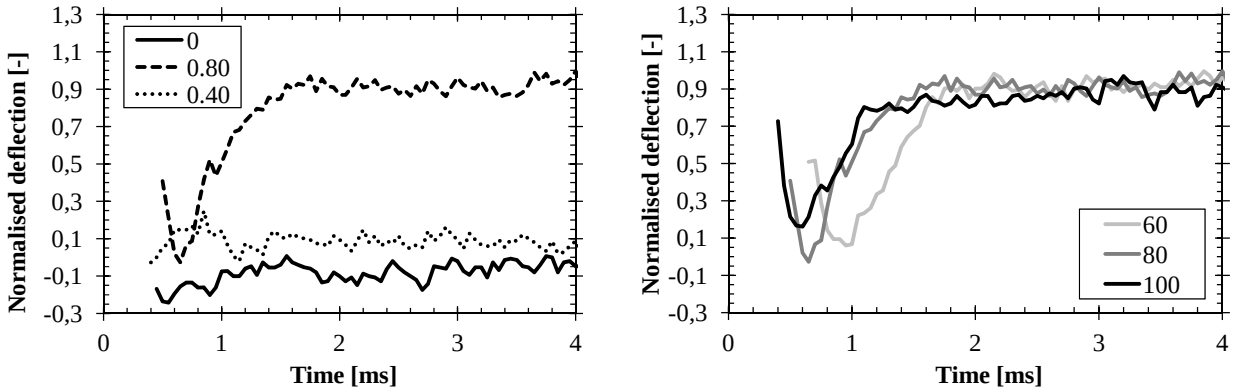

Figure 13 Transient behaviour of the spray axis for three different eccentricities (left) and at maximum eccentricity for three different rail pressures (right).

Conclusions

The investigations confirm the findings of earlier pre-tests, in that the arrangement of the orifice relative to the central bore of the injector has a non-negligible impact on spray morphology; specifically, if non-negligible eccentricity levels are applied. In order to quantitatively assess such effects, a dedicated test setup has been realised, including the development and application of tailor-made data processing routines.

The key results of the present study can be summarised as follows:

- Fuel sprays in large diesel engines are basically non-symmetric. The rather elliptic shape of their cross-section is becoming even more pronounced with increased eccentricity.
- The eccentric arrangement of an orifice results in a deflection of the axis of a fully established spray from its nominal orientation, not only in the plane of the eccentricity but also in the direction perpendicular to it, with maximum deflection levels in the range of 10°. This is an additional confirmation of the complex three-dimensional structure of sprays at such conditions.
- The deflection increases as a function of eccentricity of the nozzle hole and is trendwise reduced with increasing injection pressure. The geometry of the central bore of the injector has an additional impact on the morphology of the spray.
- With high levels of eccentricity, a clear pattern can be discerned in the initial evolution of the spray deflection: Starting from a slight deflection in the direction of the eccentricity, the spray axis moves first to its nominal direction and then gradually changes orientation again towards the level of stabilisation.

The present results already provide an excellent basis for the better understanding of phenomena observed in large diesel engine combustion systems; however, further investigations are needed in order to explain in more detail and appropriately model the effects associated with injector geometry and injection parameter variations. For this purpose, both more in-depth experimental studies and computational investigations of the fluid dynamic aspects of injection systems are required.

Acknowledgements

The present work has been conducted as part of the HERCULES-C project within EC's 7th Framework Program, Contract SCP1-GA-2011-284354. Additional financial support by the Swiss Federal Government (SFOE Contract 154269, Project 103241) is gratefully acknowledged. The authors thank Mr. Aleš Srna for his valuable support during the measurement campaign.

References

[1] Hensel S., Herrmann K., Schulz R. and Weisser G., COMODIA 2012, Fukuoka, Japan.
[2] Schulz R., Hensel S., von Rotz B., Schmid A., Herrmann K. and Weisser G., CIMAC 2013, Paper No. 259, Shanghai, China, 2013.
[3] Herrmann K., Schulz R. and Weisser G., CIMAC 2007, Vienna, Austria, 2007.
[4] Herrmann K., Kyrtatos A., Schulz R. and Weisser G., ICLASS 2009, Vail, Colorado, 2009.
[5] Herrmann K., von Rotz B., Schulz R., Weisser G., Boulouchos K. and Schneider B., ILASS 2010, Brno, Czech Republic, 2010.
[6] Hiroyasu H. and Arai M., SAE 900475 (1990).
[7] Naber J.D. and Siebers D.L., SAE 960034 (1996).
[8] von Rotz B., Herrmann K., Weisser G., Cattin M., Bolla M. and Boulouchos K., ILASS 2011, Estoril, Portugal, 2011.